Combining a Nitrogenase Scaffold and a Synthetic Compound into an Artificial Enzyme

Kazuki Tanifuji, Chi Chung Lee, Yasuhiro Ohki, Kazuyuki Tatsumi, Yilin Hu,* and Markus W. Ribbe*

Abstract: *Nitrogenase catalyzes substrate reduction at its cofactor center ([(Cit)MoFe$_7$S$_9$C]$^{n-}$; designated M-cluster). Here, we report the formation of an artificial, nitrogenase-mimicking enzyme upon insertion of a synthetic model complex ([Fe$_6$S$_9$(SEt)$_2$]$^{4-}$; designated Fe$_6^{RHH}$) into the catalytic component of nitrogenase (designated NifDK^{apo}). Two Fe$_6^{RHH}$ clusters were inserted into NifDK^{apo}, rendering the conformation of the resultant protein (designated NifDK^{Fe}) similar to the one upon insertion of native M-clusters. NifDK^{Fe} can work together with the reductase component of nitrogenase to reduce C$_2$H$_2$ in an ATP-dependent reaction. It can also act as an enzyme on its own in the presence of Eu^{II}DTPA, displaying a strong activity in C$_2$H$_2$ reduction while demonstrating an ability to reduce CN$^-$ to C$_1$–C$_3$ hydrocarbons in an ATP-independent manner. The successful outcome of this work provides the proof of concept and underlying principles for continued search of novel enzymatic activities based on this approach.*

Nitrogenase is a structurally complex and functionally versatile metalloenzyme that catalyzes the reduction of a variety of substrates, including dinitrogen (N$_2$), acetylene (C$_2$H$_2$), cyanide ions (CN$^-$), carbon monoxide (CO), and carbon dioxide (CO$_2$), under ambient conditions.[1–7] Among these reactions, the reduction of N$_2$ to ammonia (NH$_3$) represents a key step in the global nitrogen cycle, whereas the conversion of CN$^-$, CO, and CO$_2$ to hydrocarbons provides an important template for future development of strategies to recycle carbon wastes into useful carbon fuels.[8,9] The "conventional" molybdenum (Mo)-nitrogenase consists of two component proteins: a γ$_2$-dimeric reductase (designated NifH), which houses a subunit-bridging [Fe$_4$S$_4$] cluster and an ATP-binding site within each subunit; and a α$_2$β$_2$-tetrameric catalytic component (designated NifDK), which contains a P-

cluster ([Fe$_8$S$_7$]) at the α/β-subunit interface and an M-cluster ([(Cit)MoFe$_7$S$_9$C]; Cit, homocitrate) within each α-subunit (Figure S1 A, Supporting Information). Catalysis by Mo-nitrogenase is enabled by the formation of a functional complex between NifH and NifDK,[10] and the subsequent ATP-dependent transfer of electrons from the [Fe$_4$S$_4$] cluster of NifH, via the P-cluster, to the M-cluster of NifDK, where substrate reduction occurs (see Figure S1 A).

The M-cluster ([(Cit)MoFe$_7$S$_9$C]$^{n-}$) can be viewed as [MoFe$_3$S$_3$] and [Fe$_4$S$_3$] subclusters bridged by three μ$_2$-"belt" sulfur (S) atoms and a μ$_6$-interstitial carbide (C^{4-}) atom; in addition, it is coordinated by an organic compound, homocitrate, at its Mo end (Figure 1 A).[11–13] This unique metallocluster has attracted the attention of synthetic chemists and chemical biologists alike and prompted a joint search between
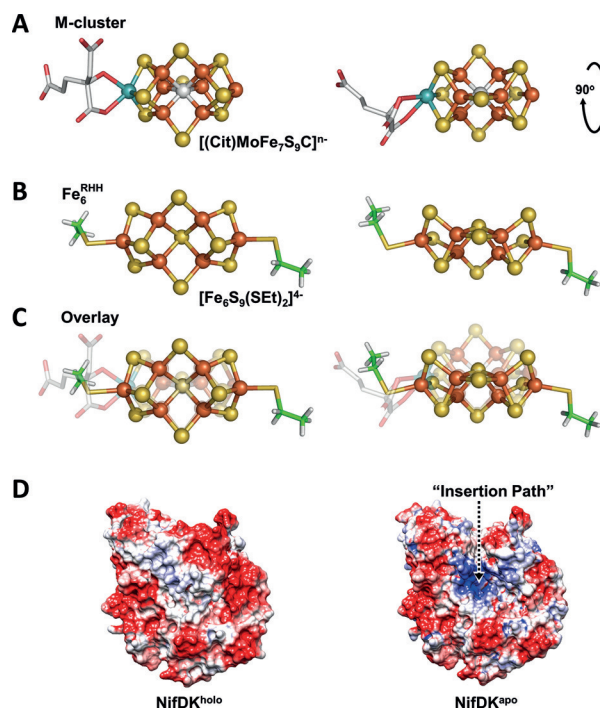

Figure 1. Nitrogenase cofactor, synthetic compound, and protein scaffold. Structural models of A) the M-cluster and B) the Fe$_6^{RHH}$ compound, and C) the overlay of the two structures in top (left) and side (right) views. PDB entry 3U7Q[12] and data from Ref. [15] were used to generate these models. Fe, orange; S, yellow; Mo, cyan; O, red; C (M-cluster), light gray; C (Fe$_6^{RHH}$), green; H (Fe$_6^{RHH}$), gray. D) Comparison of the α-subunits of the wild-type NifDK (NifDK^{holo}) and the cofactor-deficient NifDK (NifDK^{apo}), which reveals the presence of a positively charged cofactor-insertion path in NifDK^{apo} (right) that is closed up in NifDK^{holo} upon insertion of the cofactor (left).

[*] Dr. K. Tanifuji, Dr. C. C. Lee, Prof. Dr. Y. Hu, Prof. Dr. M. W. Ribbe
    Department of Molecular Biology and Biochemistry, University of California, Irvine
    Irvine, CA 92697-3900 (USA)
    E-mail: yilinh@uci.edu
             mribbe@uci.edu
    Prof. Dr. Y. Ohki, Prof. Dr. K. Tatsumi
    Department of Chemistry, Graduate School of Science and Research Center for Materials Science, Nagoya University
    Furo-cho, Chikusa-ku, Nagoya 464-8602 (Japan)
    Prof. Dr. M. W. Ribbe
    Department of Chemistry, University of California, Irvine
    Irvine, CA 92697-2025 (USA)

them for a synthetic mimic of the M-cluster that could be combined with an appropriate protein scaffold into a functional enzyme. One synthetic compound has come into sight as a potential candidate for this line of investigation. First reported by the Holm group in 1981, this $[Fe_6S_9(SEt)_2]^{4-}$ cluster (designated Fe_6^{RHH}) is a hexanuclear, dithiolate Fe–S cluster with non-cuboidal geometry and rhomb faces.[14,15] Compared to the M-cluster (Figure 1 A; also see Figure S2), Fe_6^{RHH} has a Fe atom substituting for the Mo atom and the homocitrate moiety at one end of the cluster; moreover, it "misses" two μ_4-Fe atoms and has a μ_4-bridging S atom instead of the μ_6-interstitial C atom in the "center" of the cluster (Figure 1 B; also see Figure S2). Strikingly, despite these differences, Fe_6^{RHH} bears a remarkable resemblance to the M-cluster in the overall geometry, overlaying well with the structure of the M-cluster except for the absence of one of the three "Fe faces" of the cofactor (Figure 1 C). Additionally, the anionic nature of Fe_6^{RHH} mimics that of the M-cluster, which is believed to be crucial for incorporation of the cofactor along a positively charged insertion path into NifDK (Figure 1 D).[16] Finally, Fe_6^{RHH} is known to undergo facile ligand substitutions,[14,15] which could facilitate exchange of the ethanethiol ligand of Fe_6^{RHH} with the M-cluster ligands, $Cys^{\alpha 275}$ and $His^{\alpha 442}$, at the cofactor-binding site of NifDK.

Indeed, Fe_6^{RHH} could be inserted into the cofactor-deficient form of NifDK (designated $NifDK^{apo}$), resulting in an artificial catalytic component of nitrogenase with a synthetic cofactor center. Metal analysis revealed an increase of the Fe content from (15.2 ± 1.4) to (27.2 ± 0.1) mol Fe/mol protein before and after $NifDK^{apo}$ was incubated with Fe_6^{RHH} (Table S1), suggesting the formation of a Fe_6^{RHH}-reconstituted form of NifDK (designated $NifDK^{Fe}$) upon such a treatment. Subtraction of the Fe content of $NifDK^{apo}$ (each containing two P-clusters) from that of $NifDK^{Fe}$ (each containing two P-clusters plus two Fe_6^{RHH}) indicated "acquisition" of approximately 12 mol Fe/mol protein by $NifDK^{Fe}$, which would be consistent with the incorporation of two Fe_6^{RHH} (each containing six Fe atoms) into the two cofactor-binding sites in NifDK (Figure S1 A). Treatment of $NifDK^{Fe}$ and $NifDK^M$ (i.e., an M-cluster-reconstituted form of NifDK) by an iron chelator, bathophenanthroline disulfonate, resulted in chelation of (12.3 ± 0.7) and (12.2 ± 1.1) mol Fe/mol protein, respectively. These chelation-accessible Fe atoms likely originated from the unprotected Fe atoms of the P-cluster, particularly given the relatively exposed location of this cluster at the α/β-subunit interface of NifDK (Figure S1 A). More importantly, the nearly identical amounts of accessible Fe atoms in $NifDK^{Fe}$ and $NifDK^M$ implied that the two proteins had similar flexibility in the protein environments surrounding the clusters that rendered the accessibility of the cluster Fe atoms similar to that of the Fe chelator. One reason for such a similarity could be a similar conformation assumed by the two proteins upon incorporation of their respective cofactors. In this scenario, $NifDK^{Fe}$ and $NifDK^M$ could form similar complexes with NifH, which would enable analogous ATP-dependent electron transfer within the complexes for the subsequent substrate reduction at their respective cofactor sites (Figure S1 A).
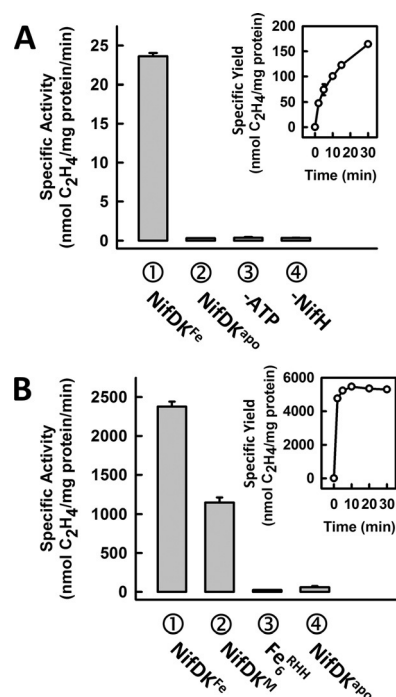

Figure 2. C_2H_2 reduction by $NifDK^{Fe}$ in ATP-dependent and independent reactions. A) Specific activity of C_2H_4 formation by $NifDK^{Fe}$ (①) or $NifDK^{apo}$ (②) from C_2H_2 reduction in an assay containing NifH, ATP, and dithionite; or by $NifDK^{Fe}$ in the same assay minus ATP (③) or NifH (④). The inset shows the time course of ATP-dependent C_2H_4 formation by $NifDK^{Fe}$. B) Specific activity of C_2H_4 formation by $NifDK^{Fe}$ (①), $NifDK^M$ (②), Fe_6^{RHH} (③), or $NifDK^{apo}$ (④) from C_2H_2 reduction in an assay containing $Eu^{II}DTPA$. The inset shows the time course of ATP-independent C_2H_4 formation by $NifDK^{Fe}$. Data are shown as mean $\pm$ SD ($N = 3$).

Consistent with this suggestion, $NifDK^{Fe}$ was capable of reducing acetylene (C_2H_2) to ethylene (C_2H_4) when it was combined with NifH, ATP and dithionite (Figure 2 A, ①), forming 164 nmol C_2H_4/mg protein (equivalent to 36 turnovers) over a time period of 30 min (Figure 2 A, inset). This activity originated from Fe_6^{RHH}, as no activity was observed prior to insertion of Fe_6^{RHH} into $NifDK^{apo}$ (Figure 2 A, ②). Furthermore, $NifDK^{Fe}$ was inactive in the C_2H_2 reduction when ATP (Figure 2 A, ③) or NifH (Figure 2 A, ④) was omitted. The specific activity of ATP-dependent C_2H_2 reduction by $NifDK^{Fe}$ ((23.7 ± 0.4) nmol C_2H_4/mg protein/min) was only 2% of the activity upon reduction by $NifDK^M$ ((1057 ± 55) nmol C_2H_4/mg protein/min), reflecting a structural/redox difference between Fe_6^{RHH} and the M-cluster (Figure 1) and/or an "imperfect" alignment of Fe_6^{RHH} with other components along the electron transfer pathway upon docking of NifH on $NifDK^{Fe}$ (Figure S1 A). Nevertheless, the observed ATP- and reductase-dependence, as well as the ability to reduce C_2H_2, established $NifH/NifDK^{Fe}$ as a two-component enzymatic system analogous to the native nitrogenase (i.e., NifH/$NifDK^M$). Interestingly, when combined with $Eu^{II}DTPA$ (DTPA = diethylene triamine pentaacetic acid) ($E^0 = -1.14$ V at pH 8) in an aqueous buffer, $NifDK^{Fe}$ was able to catalyze the reduction of C_2H_2 to C_2H_4 much more efficiently in the absence of ATP and NifH (Figure 2 B, ①), forming 4758 nmol C_2H_4/mg protein within the first 2 min and reach-

ing a maximum product formation of 5460 nmol C_2H_4/mg protein (equivalent to 1213 turnovers) over a time period of 10 min (Figure 2B, inset). Neither Fe_6^{RHH} (Figure 2B, ③) nor $NifDK^{apo}$ (Figure 2B, ④) alone showed C_2H_2 reduction in the $Eu^{II}DTPA$-driven reaction, suggesting that the activity was achieved only upon incorporation of Fe_6^{RHH} into NifDK. Moreover, $NifDK^{Fe}$ was twice as active as $NifDK^M$ in ATP-independent C_2H_2 reduction (Figure 2B, ②), showing an activity normally achieved by the wild-type NifDK in ATP-dependent C_2H_2 reduction.[17] Together, these observations demonstrated the ability of $NifDK^{Fe}$ to function as an efficient, artificial C_2H_2 reductase on its own (Figure S1B).

The observation of strong reactivity of $NifDK^{Fe}$ toward C_2H_2 compelled us to further explore the reactivity of this artificial enzyme toward other carbon-containing compounds, such as cyanide ions (CN^-), in ATP-independent reactions. Driven by $Eu^{II}DTPA$, $NifDK^{Fe}$ was capable of reducing CN^- to C_1–C_3 hydrocarbons at a total of 168 nmol reduced C/mg protein (equivalent to 37 turnovers) over a time period of 90 min (Figure 3A, ●); in contrast, no hydrocarbon product was generated by $NifDK^{apo}$ in the same, $Eu^{II}DTPA$-driven reaction (Figure 3A, ○), suggesting that the activity of CN^- reduction was associated with the NifDK-bound Fe_6^{RHH}. GC–MS analysis further confirmed CN^- as the source of carbon in the hydrocarbon products, showing expected mass shifts of +1, +2, and +3, respectively, of C_1 (CH_4), C_2 (C_2H_4, C_2H_6), and C_3 (C_3H_6, C_3H_8) products upon substitution of $^{13}CN^-$ for $^{12}CN^-$ (Figure 3B, top vs. bottom). It is interesting to note that reduction of CN^- to hydrocarbons by $NifDK^{Fe}$ was accompanied by simultaneous formation of NH_4^+; however, the amount of N in NH_4^+ ((8.1 ± 1.1) nmol N/mg protein/min) was 1.8-fold in excess (as opposed to being equivalent) to the total amount of C in hydrocarbon products that were detected in this reaction ((4.4 ± 0.6) nmol reduced C/mg protein/min). IC–MS analysis indicated that all detected NH_4^+ was generated from the reduction of CN^- (Figure S3), suggesting the

formation of other carbon-containing products (up to 44%) that remained to be identified to complete the total C count of CN^--reduction.

The results of this study provide the first proof of concept for combining a nitrogenase protein scaffold with a complex, synthetic metal–sulfur cofactor into an artificial enzyme. While this case deals specifically with a "nitrogenase mimic", several "compatibility parameters"—such as the electrostatic interaction that facilitates insertion of Fe_6^{RHH} along the cofactor-insertion path, the suitable geometry that permits occupancy of Fe_6^{RHH} at the cofactor-binding site, and the appropriate ligands that undergo facile exchange and consequently enable coordination of Fe_6^{RHH} by protein ligands—represent some general principles that are most important for the success of this line of work. With regard to the $NifDK^{apo}$ scaffold, it not only protects and stabilizes Fe_6^{RHH} in aqueous solutions, but also gives the protein-bound Fe_6^{RHH} a certain substrate selectivity that is characteristic of enzymatic systems. As far as Fe_6^{RHH} is concerned, it was shown to undergo a reversible one-electron transfer at -0.38 V vs. SHE and an irreversible one-electron transfer at -1.42 V vs. SHE in DMSO;[14,15] the oxidation states of its Fe atoms were described as $4Fe^{III}$ and $2Fe^{II}$, with electrons delocalized among these atoms.[14,18] Interestingly, these parameters are loosely analogous to those of the solvent-extracted M-cluster,[19–21] further highlighting an inherent structural–functional analogy between the two clusters.

Despite the absence of one "Fe face", Fe_6^{RHH} still "retains" two μ_2-S atoms that have a similar spatial arrangement to that of the μ_2-"belt" S atoms of the M-cluster; moreover, it has a μ_4-S atom that occupies a similar location to that of the μ_6-"central" C atom in the M-cluster (Figure 1C). Preservation of these features may be crucial for the reactivity of Fe_6^{RHH}, as a recent crystallographic study revealed displacement of a "belt" S atom by a CO moiety upon binding of CO to the M-cluster,[22] an event requiring the presence of the interstitial C atom to maintain the structural integrity of the M-cluster when the S "belt" undergoes significant rearrangement during catalysis. Thus, by analogy, the equivalents to the "belt" S and "central" C atoms in Fe_6^{RHH} may make it capable of interacting with substrates in an analogous manner to that of the M-cluster; in particular, such an analogy could explain the reactivity of Fe_6^{RHH} toward CN^-, which parallels the reactivity of the M-
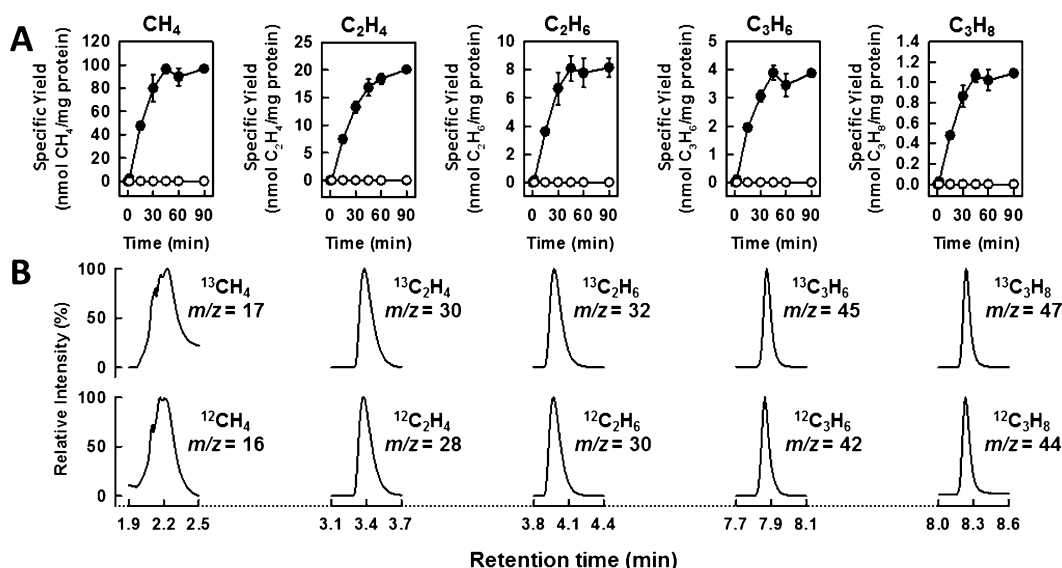

Figure 3. ATP-independent CN^- reduction by $NifDK^{Fe}$. A) Time courses of $NifDK^{Fe}$-catalyzed hydrocarbon formation by CN^- reduction in an assay containing $Eu^{II}DTPA$. B) GC–MS analysis of hydrocarbon products formed by $NifDK^{Fe}$ in the presence of $Eu^{II}DTPA$ when $^{13}CN^-$ (top) or $^{12}CN^-$ (bottom) was supplied as a substrate.

cluster toward CO (an isoelectric molecule to the CN^- ion), in reductive C−C coupling.[2–4] On the other hand, the unique structural features of Fe_6^{RHH} result in the distinct catalytic profile of $NifDK^{Fe}$, such as improved activities of C_2H_2- and CN^--reduction when it acts on its own as an enzyme. It is conceivable, therefore, that a continued effort to incorporate other synthetic cofactor variants into a suitable protein scaffold will not only advance mechanistic understanding of nitrogenase from a different viewpoint, but also facilitate identification of novel enzymatic activities that may be useful in a practical vein.

The Fe_6^{RHH} cluster came from a long line of synthetic compounds that were generated in a quest for synthetic routes to nitrogenase-based, biomimetic metal clusters.[7,23–25] Such a quest began even before the structures of the nitrogenase clusters were known, when a variety of relatively small FeS clusters, including cubane-type FeS clusters with various ligands (and, in some cases, heterometals), were synthesized and characterized.[15,23] As chemical and spectroscopic information of the nitrogenase clusters became available, much effort has been focused on the generation of high-nuclearity metalloclusters. The previously synthesized MoFeS and VFeS clusters with phosphine ligands were utilized as instrumental building blocks in a fusion strategy that led to edge-bridged double-cubane clusters[23,24] and, subsequently, core conversion and ligand exchange/removal strategies were developed that resulted in P^N- and M-type topologs.[7] The successful synthesis of these clusters not only provides the much-needed model compounds that mimic the nitrogenase clusters in structural and redox properties, but also reveals a certain parallelism between the classic synthetic strategy[24,25] and the biosynthetic mechanisms utilized by nitrogenase clusters[26] in fusing small FeS units into larger FeS cores. A similar concept was successfully applied to the generation of a functional, semisynthetic hydrogenase.[27,28] Interestingly, a different synthetic approach emerged in recent years, which led to synthesis of a series of FeS clusters, including two 8Fe mimics of nitrogenase clusters, via spontaneous condensation of iron and sulfido monomeric units.[25] The observation of two different synthetic strategies leads to the speculation of whether the "prototype" of nitrogenase clusters originated from spontaneous reactions in the primordial, abiotic environment, which then evolved into a well-organized, protein scaffold-assisted mechanism that step-by-step fused small FeS units into high-nuclearity FeS clusters. Regardless of what evolutionary implications they may have, the chemical synthetic approaches will continue to evolve and add new members to the library of synthetic cofactors, assisting in our pursuit of artificial enzymes while providing relevant insights into the assembly and catalytic properties of nitrogenase.

Acknowledgements

[1] B. K. Burgess, D. J. Lowe, *Chem. Rev.* **1996**, *96*, 2983–3012.
[2] C. C. Lee, Y. Hu, M. W. Ribbe, *Science* **2010**, *329*, 642.
[3] Y. Hu, C. C. Lee, M. W. Ribbe, *Science* **2011**, *333*, 753–755.
[4] C. C. Lee, Y. Hu, M. W. Ribbe, *Angew. Chem. Int. Ed.* **2015**, *54*, 1219–1222; *Angew. Chem.* **2015**, *127*, 1235–1238.
[5] J. G. Rebelein, Y. Hu, M. W. Ribbe, *Angew. Chem. Int. Ed.* **2014**, *53*, 11543–11546; *Angew. Chem.* **2014**, *126*, 11727–11730.
[6] B. M. Hoffman, D. Lukoyanov, Z. Y. Yang, D. R. Dean, L. C. Seefeldt, *Chem. Rev.* **2014**, *114*, 4041–4062.
[7] S. C. Lee, W. Lo, R. H. Holm, *Chem. Rev.* **2014**, *114*, 3579–3600.
[8] C. K. Rofer-DePoorter, *Chem. Rev.* **1981**, *81*, 447–474.
[9] D. L. Gerlach, N. Lehnert, *Angew. Chem. Int. Ed.* **2011**, *50*, 7984–7986; *Angew. Chem.* **2011**, *123*, 8133–8135.
[10] D. C. Rees, F. A. Tezcan, C. A. Haynes, M. Y. Walton, S. Andrade, O. Einsle, J. B. Howard, *Philos. Trans. R. Soc. A* **2005**, *363*, 971–984.
[11] K. M. Lancaster, M. Roemelt, P. Ettenhuber, Y. Hu, M. W. Ribbe, F. Neese, U. Bergmann, S. DeBeer, *Science* **2011**, *334*, 974–977.
[12] T. Spatzal, M. Aksoyoglu, L. Zhang, S. L. Andrade, E. Schleicher, S. Weber, D. C. Rees, O. Einsle, *Science* **2011**, *334*, 940.
[13] J. A. Wiig, Y. Hu, C. C. Lee, M. W. Ribbe, *Science* **2012**, *337*, 1672–1675.
[14] G. Christou, R. H. Holm, M. Sabat, J. A. Ibers, *J. Am. Chem. Soc.* **1981**, *103*, 6269–6271.
[15] K. S. Hagen, A. D. Watson, R. H. Holm, *J. Am. Chem. Soc.* **1983**, *105*, 3905–3913.
[16] B. Schmid, M. W. Ribbe, O. Einsle, M. Yoshida, L. M. Thomas, D. R. Dean, D. C. Rees, B. K. Burgess, *Science* **2002**, *296*, 352–356.
[17] R. R. Eady, *Chem. Rev.* **1996**, *96*, 3013–3030.
[18] H. Strasdeit, B. Krebs, G. Henkel, *Inorg. Chem.* **1984**, *23*, 1816–1825.
[19] F. A. Schultz, S. F. Gheller, B. K. Burgess, S. Lough, W. E. Newton, *J. Am. Chem. Soc.* **1985**, *107*, 5364–5368.
[20] B. K. Burgess, *Chem. Rev.* **1990**, *90*, 1377–1406.
[21] T. V. Harris, R. K. Szilagyi, *Inorg. Chem.* **2011**, *50*, 4811–4824.
[22] T. Spatzal, K. A. Perez, O. Einsle, J. B. Howard, D. C. Rees, *Science* **2014**, *345*, 1620–1623.
[23] S. C. Lee, R. H. Holm, *Proc. Natl. Acad. Sci. USA* **2003**, *100*, 3595–3600.
[24] S. C. Lee, R. H. Holm, *Chem. Rev.* **2004**, *104*, 1135–1158.
[25] Y. Ohki, K. Tatsumi, *Z. Anorg. Allg. Chem.* **2013**, *639*, 1340–1349.
[26] M. W. Ribbe, Y. Hu, K. O. Hodgson, B. Hedman, *Chem. Rev.* **2014**, *114*, 4063–4080.
[27] J. Esselborn, C. Lambertz, A. Adamska-Venkatesh, T. Simmons, G. Berggren, J. Noth, J. Siebel, A. Hemschemeier, V. Artero, E. Reijerse, M. Fontecave, W. Lubitz, T. Happe, *Nat. Chem. Biol.* **2013**, *9*, 607–609.
[28] G. Berggren, A. Adamska, C. Lambertz, T. R. Simmons, J. Esselborn, M. Atta, S. Gambarelli, J. M. Mouesca, E. Reijerse, W. Lubitz, T. Happe, V. Artero, M. Fontecave, *Nature* **2013**, *499*, 66–69.